J. Mt. Sci. (2011) 8: 246–260
DOI: 10.1007/s11629-011-2105-8

Spatial Distribution of Large-scale Landslides Induced by the 5.12 Wenchuan Earthquake

XU Qiang*, ZHANG Shuai, LI Weile

State Key Laboratory of Geohazard Prevention and Geoenvironment Protection, Chengdu University of Technology, Chengdu 610059, China

**Corresponding author, e-mail: xuqiang_68@126.com*

Abstract: The 5.12 Wenchuan Earthquake in 2008 induced hundreds of large-scale landslides. This paper systematically analyzes 112 large-scale landslides (surface area > 50000 m^2), which were identified by interpretation of remote sensing imagery and field investigations. The analysis suggests that the distribution of large-scale landslides is affected by the following four factors: (a) distance effect: 80% of studied large-scale landslides are located within a distance of 5 km from the seismic faults. The farther the distance to the faults, the lower the number of large-scale landslides; (b) locked segment effect: the large-scale landslides are mainly located in five concentration zones closely related with the crossing, staggering and transfer sections between one seismic fault section and the next one, as well as the end of the NE fault section. The zone with the highest concentration was the Hongbai-Chaping segment, where a great number of large-scale landslides including the two largest landslides were located. The second highest concentration of large-scale landslides was observed in the Nanba-Donghekou segment at the end of NE fault, where the Donghekou landslide and the Woqian landslide occurred; (c) Hanging wall effect: about 70% of the large-scale landslides occurred on the hanging wall of the seismic faults; and (d) direction effect: in valleys perpendicular to the seismic faults, the density of large-scale landslides on the slopes facing the seismic wave is obviously higher than that on the slopes dipping in the same direction as the direction of propagation of the seismic wave. Meanwhile, it is found that the sliding and moving directions of large-scale landslides are related to the staggering direction of the faults in each section. In Qingchuan County where the main fault activity was horizontal twisting and staggering, a considerable number of landslides showed the feature of sliding and moving in NE direction which coincides with the staggering direction of the seismic faults.

Keywords: 5.12 Wenchuan Earthquake; Landslides; Distribution pattern; Direction effect; Locked segment effect

Received: 10 November 2010
Accepted: 30 December 2010

Introduction

The spatial distribution of earthquake-induced landslides has gained much attention from researchers and several patterns of spatial distribution have been proposed (Champati 2009; Hasi et al. 2010; Jibson et al. 1998; McCrink & Real 1996). Based on the study of the distribution of landslides induced by the Iwate-Miyagi Inland Earthquake, Hasi et al. (2010) concluded that 97.1% of the landslides occurred on the hanging wall of the seismic fault and that the number and scale of landslides tended to decrease with the increase in the distance from the seismic fault. In the case of the Chuetsu and the Chuetsu-offshore Earthquake in Japan, the landslides tended to occur in an area which was composed of an alternation of sandstone and mudstone rather than mudstone alone, and the number and magnitude of

landslides seemed to decrease with increasing distance from the seismic fault (Hasi et al. 2010). Based on the investigation in temporal satellite imagery of the 8 October 2005 earthquake in Kashmir Himalaya, Champati (2009) indicated that major lithological units such as the Subathu and Murree formations had a high vulnerability to landsliding. Garcia-Rodriguez (2008) evaluated the probability of landslide occurrence due to earthquake for El Salvador with GIS with a logistic regression model and showed that the terrain roughness and soil type were the key factors influencing landslide distribution. Jibson et al. (1998), McCrink & Real (1996) argued that slopes between 0º and 10º had a very low susceptibility to earthquake-induced failures based on the evaluation with the Newmark method for mapping earthquake-induced landslide hazards in the Laurel quadrangle (7.5Ms), Santa Cruz County, California. Jibson et al. (1998) presented a mapping method based on GIS which directly presents the distribution of landslides triggered by earthquakes and their probability of failure. Cole (1998) compared the behavior of two reactivated landslides during an earthquake with the results of slope-stability calculations, and tested the sensitivity of key parameters in the stability calculations. He came to the conclusion that the key factor is the angle of internal friction, a parameter that is difficult to determine accurately in the laboratory. Keefer (1984) analyzed a sample of 40 historical earthquakes and identified several materials that are especially susceptible to earthquake induced landslides. Table 1 summarizes the distribution features of landslides induced by several historical earthquake events based on the literature review.

The huge 5.12 Wenchuan earthquake in 2008 is characterized by high magnitude (8.0 Ms), shallow hypocenter (the depth of the hypocenter was less than 20 km), long fracture zone (approximately 300 km), strong staggering (the biggest staggering displacement was about 7m), large energy release (three times the energy of the 1976 Tangshan earthquake (7.7Ms)), and long duration (the duration of the main shock was about 120s). Due to the weak geological environment in the Longmen Mountain Range, the Wenchuan Earthquake caused thousands of landslides with various sizes in terms of displaced volume (Xu et al. 2009). Westen et al. (2010) mapped nearly 60,000 landslide scarps for the area hit by the Wenchuan Earthquake by using a large set of high resolution satellite images for both the pre- and post-earthquake situations. They concluded that the landslide density in areas where the fault had mainly a thrust component with a low angle fault plane was much higher than that in the areas with steeper fault angles and a major strike slip component. Hundreds of large-scale landslides induced by the Wenchuan Earthquake showed special characteristics differing from the usual slope instability phenomena such as the hyperdynamic features, with large scale high-speed projecting phenomena and long distance flow movements (Xu et al. 2008, 2009; Huang et al. 2008a, 2008b, 2009; Wang 2010). Sato et al. (2009) mapped earthquake-induced landslides

Table 1 Summary of distribution rule of landslides induced by historical earthquake

NO.	Earthquake name	Landslide distribution feature
1	Iwate-Miyagi Inland Earthquake	Mainly occurred on the hanging wall and the number and scale of landslides tend to decrease with an increase of the distance from the source fault (Hasi 2010)
2	Chuetsu-offshore Earthquake	Slides occurred in areas which of an alternation of sandstone and mudstone, and the landslide number and magnitude seems to decrease with the distance from the source fault (Hasi 2009)
3	Loma-Prieta Earthquake	Disrupted slides seem to correlate better with low frequency seismic waves and coherent slides with high frequency waves, and their relationship is strongly affected by the lithology of the material (Ramos-C 2009)
4	Kashmir Himalaya Earthquake	The major lithological Subath and Murree formations had a positive effect on the landslide occurrence (Champati et al. 2009)
5	EI-Salvador Earthquake	Landslide density is low in areas with terrain slopes between 0° and 10° (Garcia-Rodriguez et al. 2008)
6	North Pakistan Earthquake	100 landslide failures occurred, and many of them concentrated on the north eastern side of the Muzaffarabad fault and Tanda fault (Marui)

triggered by the Wenchuan Earthquake by using satellite imagery and Google Earth and concluded that the landslides were mainly concentrated along the Beichuan fault and the maximum spatial density of large landslides was 0.3 landslides/km^2.

It is of great significance and practical value to study the distribution of large-scale landslides triggered by the Wenchuan Earthquake in a systematical way so as to get deeper insight into the rule of earthquake triggering landslides and thus to minimize economic and social loss from the hazards. The present paper focuses on factors influencing the spatial distribution of earthquake-induced large-scale landslides in Wenchuan Earthquake area. Multi-factor analysis was employed together with GIS program to conduct the spatial modeling and qualitative analysis. The factors considered included distance, locked-segment, hanging wall and direction from both the geological and the geotechnical points of view.

1 Methodology and Input Data

The methodology used in this research consists of two main steps. The first step is to generate an inventory map of the large-scale landslides triggered by the Wenchuan Earthquake and the second step is to analyze its distribution with a set of parameters such as distance from seismic faults, slope direction etc. Three different datasets were used: (1) Pre- and post-earthquake satellite images and aerial photos; (2) pre-earthquake Digital Elevation Model (DEM); and (3) surface rupture lines triggered by the earthquake. The data analysis was carried out with ArcGIS 9.2, ENVI 4.5, and ERDAS Imagine 9.0 program.

Since most of the large-scale landslides have slided down completely during earthquake, the displaced mass was stable in general terms after the earthquake. This imposed little threat to lives and properties in the disaster area. That is the reason that site-specified field investigations were not conducted on these landslides by the relevant government departments. Due to a lack of field investigation data, the volumes of these landslides could only be estimated. However, the geometric size and surface area of each landslide can be precisely measured on the remote sensing imagery. In order to avoid any errors arising from volume estimations, the present study utilized the total surface area of the landslide source area (accumulation area and the area of the travel path) to define the size of the landslide.

The locations of the large-scale landslides were mapped from the pre- and post-earthquake satellite images and aerial photographs and the DEM of the area. Figure 1 shows the spatial coverage of the satellite images and aerial photographs that were collected for both the pre- and post-earthquake situation. The pre-earthquake images are multi-spectral data such as ASTER (15 m spatial resolution) and ALOS AVNIR-2 (10 m) and panchromatic data from ALOS PRISM (2.5 m) and the Indian Cartosat-1 (2.5 m). Post earthquake imagery includes SPOT-5 (2.5 m), IKONOS (2.5 m) and aerial photographs (0.5 m).

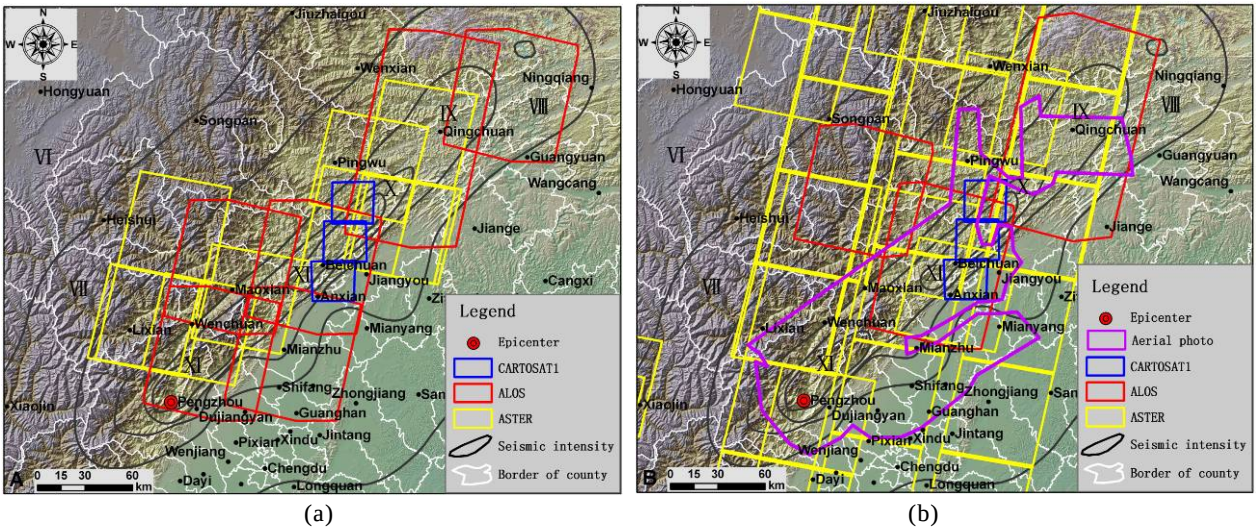

(a) (b)

Figure 1 The spatial coverage of the satellite images and aerial photos of the study area: (a) pre-earthquake; and (b) post-earthquake

The DEM was generated from digitized contour lines from 1:50 000 topographic maps with contour intervals of 20 meters for low relief areas and 50 meters for mountainous areas. The DEM was used to generate a derivative map showing the ridges and slope lengths which was helpful to detect landslides. The individual large-scale landslides were mapped as polygons.

The visual landslide interpretation was carried out on false color composites, panchromatic images or aerial photographs, using monoscopic image interpretation. Although stereoscopic image interpretation would be better for optimal landslide interpretation, it was not practically possible to generate stereo images for such a large area. In total, 112 large-scale landslides (with surface area larger than 50,000 m^2) were identified within the distance of 15 km from the seismic fault (Figure 2). The basic information of these landslides is summarized in Table 2. The longest distance from large-scale landslide to Yingxiu - Beichuan fault was approximately 13 km. The largest landslide was the Daguangbao landslide in Anxian County with a surface area of 7.27 km^2, and the smallest one was the Xiaowuji landslide in Qingchuan County.

The northeastern segment of Yingxiu-Beichuan fault, especially in the Qingchuan County, spread out into a multi-branch rupture. Field investigations show that the formation of large-scale landslides was more closely related with the Yingxiu-Beichuan secondary faults in the section from Magong to Donghekou in Qingchuan County. Therefore, for the measurement of distances, this section was based on the measured faults in Figure 2 (denoted by dotted line), in other sections the measurements were based on the surface rupture zone (black lines) given by Sichuan Provincial Seismological Bureau. It can be found from Figure 2 that in the section from Hongbai town to Chaping

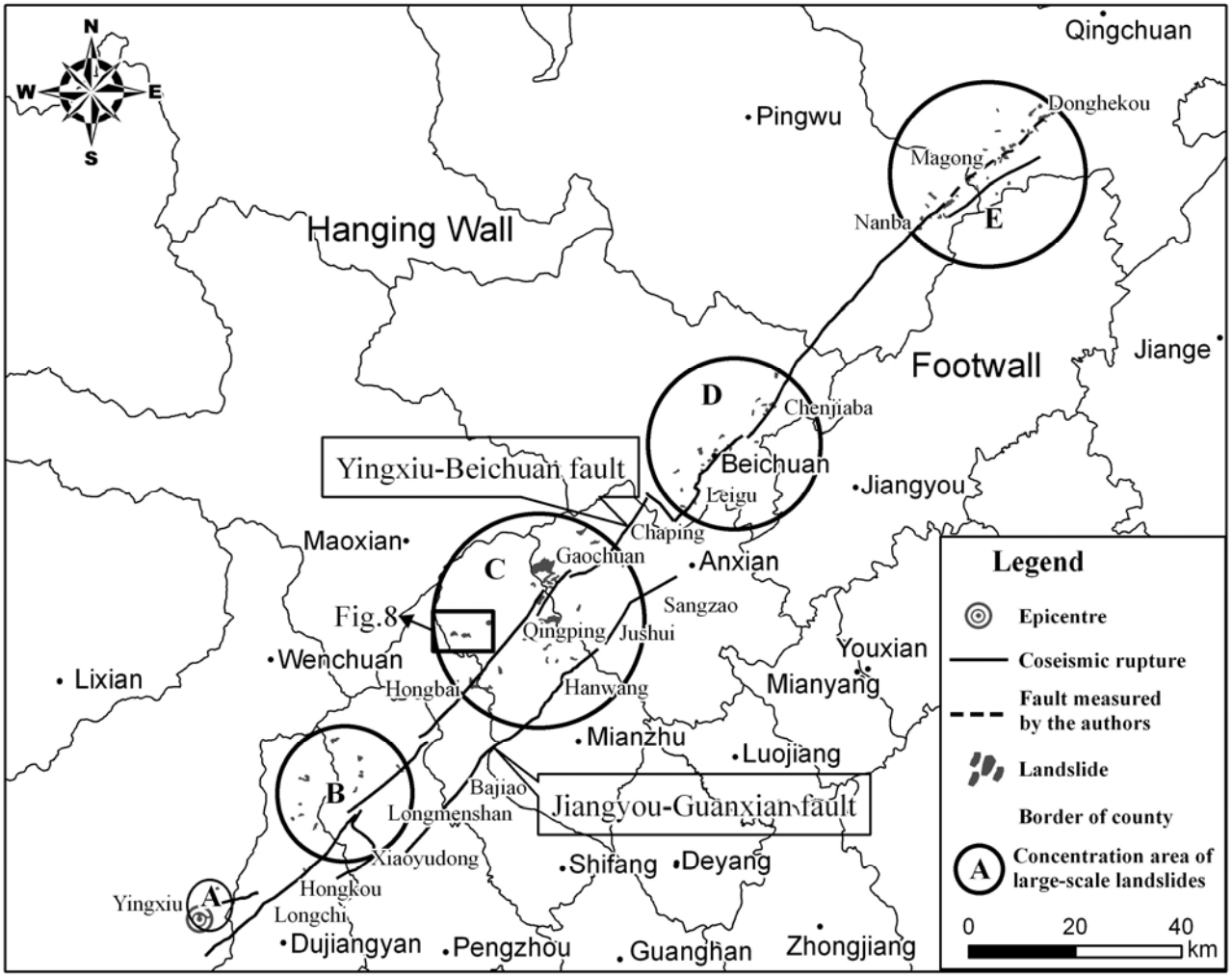

Figure 2 Distribution of large-scale landslides induced by Wenchuan Earthquake

village, the occurrence of landslides may also be related to the Jiangyou-Guanxian fracture. Because the landslides were located at the hanging wall of the front Mountain fault, it was difficult to distinguish clearly which fault was most closely related to each individual landslide. Therefore, the distances were always measured from the Yingxiu-Beichuan fault. Also, the occurrence of landslides in the section from Magong to the Donghekou in Qingchuan County may have some relation to the activities of the other branch fault (black lines in Figure 3). However, it is also difficult to determine which fault plays the major role in the occurrence of the individual landslides.

Table 2 Basic information on the large-scale landslides in the Wenchuan earthquake-hit area with surface areas larger than 50,000 m^2

No.	Landslide sites	Area (m^2)	DLF* (m)	Faultwall
1	Daguangbao, Anxian,104.121° E,31.645° N	7273719	4800	Hanging
2	Wenjiagou,Mianzhu,104.135° E,31.553° N	2945520	3900	Foot
3	Donghekou,Qingchuan,105.115° E,32.405° N	1283627	300	Hanging
4	Zhengjiagou,Pingwu,104.925° E,32.265° N	1014987	2400	Hanging
5	Shuimogou,Shifang,103.982° E,31.440° N	915608	700	Hanging
6	Dawuji,Anxian,104.197° E,31.701° N	792190	6900	Hanging
7	Woqian,Qingchuan,104.966° E,32.309° N	695672	200	Hanging
8	Dashanshu,Mianzhu,103.969° E,31.524° N	693687	6900	Hanging
9	Hongshigou,Anxian,104.133° E,31.627° N	687520	2240	Hanging
10	Bingkoushi,Pengzhou,103.713° E,31.344° N	575556	12600	Hanging
11	Tangjiashan,Beichuan,104.431° E,31.842° N	572009	2780	Hanging
12	Huatizigou,Pengzhou,104.015° E,31.546° N	541193	4980	Hanging
13	Wenjiaba,Pingwu,104.865° E,32.223° N	537101	380	Hanging
14	Niumiangou,Wenchuan,103.458° E,31.045° N	527700	300	Hanging
15	Haixingou,Mianzhu,103.946° E,31.528° N	517573	8888	Hanging
16	Maanshi,Pingwu,104.891° E,32.277° N	509836	4200	Hanging
17	Shibangoucun,Qingchuan,105.091° E,32.420° N	496983	2300	Hanging
18	Guershan,Beichuan,104.576° E,31.919° N	471112	0	Hanging
19	Xiaojiashan,Mianzhu,104.038° E,31.464° N	465899	2900	Hanging
20	Xinkaidong,Pengzhou,103.763° E,31.313° N	449685	6800	Hanging
21	Baozangcun,Anxian,104.223° E, 31.685° N	418744	4030	Hanging
22	Mianjiaogou,Beichuan,104.489° E,31.850° N	377247	550	Foot
23	Weijiashan,Beichuan,104.582° E,31.971° N	358021	2120	Hanging
24	Caochaoping,Anxian,104.138° E,31.608° N	354046	660	Hanging
25	Miepengzi3#,Mianzhu,104.119° E,31.591° N	353817	600	Hanging
26	Laoyingyan,Anxian,104.145° E,31.623° N	353242	1050	Hanging
27	Huoshigou,Anxian,104.134° E,31.615° N	322155	1400	Hanging
28	Zhangjiashan,Anxian,104.192° E,31.572° N	306576	6000	Foot
29	Macaotan,Mianzhu,104.011° E,31.434° N	305989	2700	Foot
30	Xiejiadianzi,Pengzhou,103.841° E,31.297° N	294256	1100	Hanging
31	Shibangou,Qingchuan,105.107° E,32.431° N	288305	2400	Hanging
32	Huishuituo,Pengzhou,103.764° E,31.284° N	270980	4200	Hanging
33	Dazhuping,Anxian,104.148° E,31.617° N	270692	540	Hanging
34	Miepengzi2#,Mianzhu,104.115° E,31.586° N	262520	600	Hanging
35	Heshanggou3#,Dujiangyan,103.658° E,31.281° N	257635	10400	Hanging

Table 2 Basic information on the large-scale landslides in the Wenchuan earthquake-hit area with surface areas larger than 50,000 m^2 (continued)

No.	Landslide sites	Area (m^2)	DLF* (m)	Faultwall
36	Muguapingcun,Shifang,103.990° E,31.439° N	256340	900	Foot
37	Miepengzi1#,Mianzhu,104.113° E,31.581° N	255296	600	Hanging
38	Dongxigou,Beichuan,104.474° E,31.868° N	246020	2200	Hanging
39	Yaozidong,Pingwu,104.870° E,32.239° N	242553	800	Hanging
40	Baichaping,Dujiangyan,103.676° E,31.199° N	241874	4700	Hanging
41	Changping,Pengzhou,103.754° E,31.258° N	224645	2400	Hanging
42	Paodili,Qingchuan,105.035° E,32.355° N	222157	700	Hanging
43	Xiaomuling,Mianzhu,104.101° E,31.614° N	218705	2450	Hanging
44	Heshangqiao1#,Dujiangyan,103.649° E,31.278° N	214020	10900	Hanging
45	Boshuling,Beichuan,104.384° E,31.807° N	208968	4350	Hanging
46	Dawan,Beichuan,104.535° E,31.907° N	203959	2150	Hanging
47	Baiguoshu,Beichuan,104.462° E,31.844° N	203246	1000	Hanging
48	Zengjiagou,Mianzhu,104.183° E,31.485° N	198165	11350	Foot
49	Zhangjiagou,Beichuan,104.563° E,31.912° N	196299	640	Hanging
50	Zhaojiaqu,Qingchuan,105.072° E,32.387° N	193153	1300	Hanging
51	Heitanzi,Anxian,104.193° E,31.523° N	182452	8900	Foot
52	Anleshan,Beichuan,104.398° E,31.747° N	180809	1140	Hanging
53	Yinshangou,Beichuan,104.557° E,31.921° N	177361	1300	Hanging
54	Xiaotianchi,Mianzhu,104.130° E,31.483° N	175758	8200	Foot
55	Yanyangcun,Beichuan,104.543° E,31.858° N	174008	1600	Foot
56	Shicouzi,Pingwu,104.917° E,32.242° N	169540	0	Hanging
57	Chenjiaping,Anxian,104.237° E,31.660° N	169368	1050	Hanging
58	Wangyemiao,Dujiangyan,103.631° E,31.210° N	167980	9300	Hanging
59	Jiadanwan1#,Dujiangyan,103.648° ,31.217° N	166643	7900	Hanging
60	Jinhelinkuang,Mianzhu,104.019° E,31.438° N	159848	2800	Foot
61	Fengyanzi,Beichuan,104.421° E, 31.754° N	158468	0	Foot
62	Changtan,Mianzhu,104.133° E,31.509° N	151094	6670	Foot
63	Weijiagou,Beichuan,104.436° E,31.808° N	150818	450	Hanging
64	Xiaogangjian,Mianzhu,104.126° E,31.502° N	149074	6280	Foot
65	Baiyanshan,Qingchuan,105.022° E,32.387° N	147940	4300	Hanging
66	Guoniucun,Beichuan,104.395° E,31.776° N	147554	3000	Hanging
67	Heshangqiao2#,Dujiangyan,103.659° E,31.276° N	147394	9600	Hanging
68	Bazuofen,Anxian,104.219° E,31.519° N	146272	11000	Foot
69	Tiangengli,Qingchuan,105.044° E,32.299° N	144729	1400	Foot
70	Hongmagong,Qingchuan,104.963° E,32.301° N	144683	350	Foot
71	Baiguocun,Qingchuan,105.088° E,32.384° N	139800	300	Foot
72	Huangtuliang,Beichuan,104.559° E,31.904° N	135084	550	Hanging
73	Qinglongcun,Qingchuan,105.037° E,32.342° N	134079	790	Foot
74	Pengjiashan,Beichuan,104.546° E,31.930° N	127156	2900	Hanging
75	Wangjiayan,Beichuan,104.449° E,31.826° N	125381	400	Hanging
76	Yibadao,Mianzhu,104.149° E,31.481° N	125059	9600	Foot
77	Laohuzui,Wenchuan,103.484° E,31.090° N	125039	2700	Hanging

Table 2 Basic information on the large-scale landslides in the Wenchuan earthquake-hit area with surface areas larger than 50,000 m^2 (continued)

No.	Landslide sites	Area (m^2)	DLF* (m)	Faultwall
78	Beizhongxinqu,Beichuan,104.459° E,31.830° N	124365	300	Foot
79	Xiaomeizilin,Mianzhu,104.018° E,31.401° N	122530	5800	Foot
80	Xiangshuishi,Pengzhou,103.765° E,31.290° N	119194	4600	Hanging
81	Gaojiamo,Pingwu,104.881° E,32.261° N	115301	1600	Hanging
82	Jiadanwan2#,Dujiangyan,103.645° E,31.234° N	114905	9300	Hanging
83	Dahuashu,Beichuan,104.390° E,31.730° N	113111	0	Hanging
84	Wangjiabao,Beichuan,104.401° E,31.738° N	112418	0	Hanging
85	Jiankangcun,Pingwu,104.887° E,32.242° N	111106	340	Hanging
86	Xiaojiaqiao,Anxian,104.278° E,31.646° N	110085	3000	Foot
87	Lingtou,Qingchuan,105.050° E,32.361° N	102116	800	Hanging
88	Longwancun,Beichuan,104.571° E,31.921° N	99821	650	Hanging
89	Zhangzhengbo,Qingchuan,105.017° E,32.333° N	99726	790	Foot
90	Nanyuecun,Dujiangyan,103.561° E,31.082° N	99350	0	Hanging
91	Xiajiapin,Dujiangyan,103.655° E,31.122° N	96345	790	Hanging
92	Dujiayan,Qingchuan,105.028° E,32.334° N	94769	960	Foot
93	Madiping,Qingchuan,104.997° E,32.355° N	94633	2600	Hanging
94	Maocongshan1#,Pingwu,104.906° E,32.240° N	92355	1200	Hanging
95	Yandiaowo,Qingchuan,105.099° E,32.390° N	92128	340	Foot
96	Chuanzigou,Mianzhu,104.086° E,31.518° N	91718	2200	Foot
97	Xiaoxishan,Qingchuan,105.031° E,32.359° N	90298	1000	Hanging
98	Xishanpo,Beichuan,104.436° E,31.818° N	83663	1140	Hanging
99	Hejiayuan,Qingchuan,105.020° E,32.281° N	83359	1990	Foot
100	Zhaojiashan,Qingchuan,105.041° E,32.342° N	82329	1000	Foot
101	Liushuping1#,Qingchuan,105.055° E,32.363° N	81000	780	Hanging
102	Weiziping,Qingchuan,105.083° E,32.387° N	74661	470	Hanging
103	Gongziba,Qingchuan,105.041° E,32.351° N	71221	220	Hanging
104	Maerping,Qingchuan,105.022° E,32.424° N	70982	7500	Hanging
105	Maocongshan2#,Pingwu,104.908° E,32.243° N	70252	1200	Hanging
106	Muhongping,Qingchuan,104.982° E,32.289° N	68288	2600	Foot
107	Machigai,Qingchuan,105.024° E,32.341° N	66602	500	Foot
108	Zixicun,Pingwu,104.941° E,32.276° N	57820	2400	Hanging
109	Liushuping2#,Qingchuan,105.054° E,32.365° N	54810	1000	Hanging
110	Dongjia,Qingchuan,105.031° E,32.343° N	54353	1000	Foot
111	Majiawo,Qingchuan,105.047° E,32.362° N	50591	1100	Hanging
112	Xiaowuji,Qingchuan,105.002° E,32.307° N	50122	2100	Foot
*DLF: The distance from landslide to fault				

Table 3 Statistical information on numbers of landslides in terms of distance to the source fault(s)

Distance (km)	<1	1~2	2~3	3~4	4~5	5~6	6~7	7~8	8~9	9~10	10~11	11~12	12~13
Number	44	15	22	2	8	2	5	2	3	4	3	1	1
Percentage (%)	39.3	13.4	19.6	1.8	7.1	1.8	4.5	1.8	2.7	3.6	2.7	0.9	0.9

2 Factors Affecting the Distribution of Large-scale Landslides

Huang and Li (2008, 2009) indicated that the landslides (including all sizes of landslides in the whole disaster-hit area) triggered by the Wenchuan Earthquake showed a zonal distribution along the earthquake source zone and linear distribution along the rivers. Based on the observation from Figure 2, generally speaking, the distribution of large-scale landslides induced by the Wenchuan Earthquake basically has similar features and patterns and the large-scale landslides had an even more close relation with the seismic fault.

2.1 Distance effect

Figure 3 shows the number of large-scale landslides at a number of distance intervals to the seismic fault(s). This shows that the occurrence of large-scale landslides is closely related with the distance to the Yingxiu - Beichuan fault. The relationship between the percentage of large-scale landslides (γ) and the distance (D_r) satisfies the equation: $\gamma = -37.115 D_r^{-1.306}$ with a value of $R^2=0.7379$ (Figure 3a). Figure 3b shows the accumulative percentage of large-scale landslides plotted against the distance to the Yingxiu-Beichuan Fault. More than 70% of the landslides are located within 3km distance from the seismic fault and 80% within 5km.

2.2 Locked segment effect

Figure 2 shows that the large-scale landslides tended to occur along the seismic fault. Furthermore, they were locally concentrated in the following five seismic fault areas outlined in Figure 2: (A) Yingxiu Area; (B) Xiaoyudong Area; (C) Hongbai - Chaping Area; (D) Leigu - Chenjiaba Area; and (E) Nanba – Donghekou Area. The number and the total surface areas of the large-scale landslides in each concentration area are listed in Table 4. The area percentage stands for the ratio of the total landslide surface area in each concentration area to the total area of all the 112 landslides.

As shown in Table 4, Area E ranks the first in terms of the number of landslides (39 nos.), followed by Area C (32) and Area D (23). However, in respect to the landslide covered area, Area C

Table 4 Number and surface area of large-scale landslides in concentration areas A to E

Concentrating section	A	B	C	D	E
Number of landslide	3	15	32	23	39
Number percentage (%)	2.7	13.4	28.6	20.5	34.8
Landslide area (m^2)	752089	3882305	19751262	4746898	8193964
Area percentage (%)	2	10.4	52.9	12.7	22
Average area (m^2)	250696	258820	617227	206387	210102

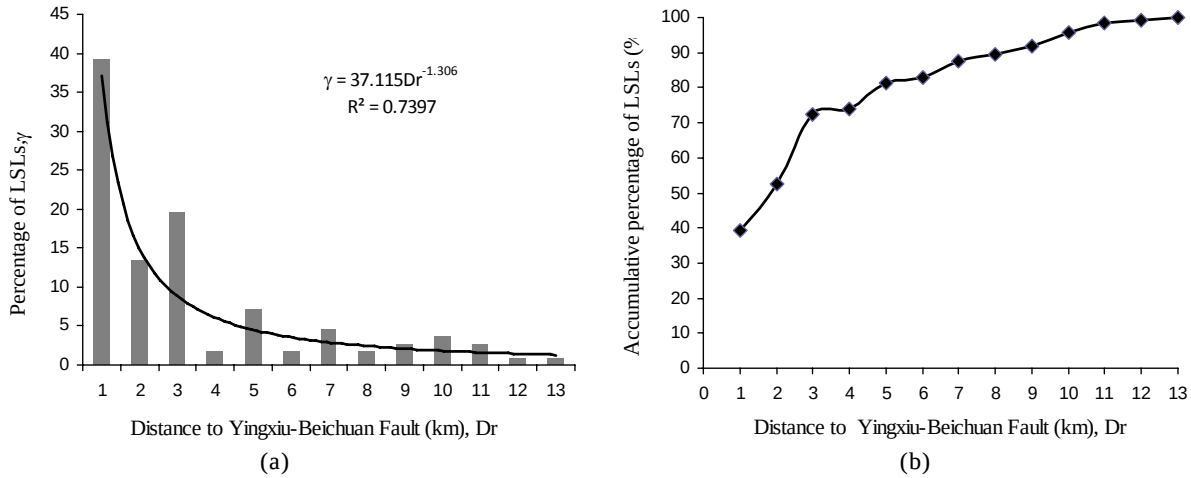

Figure 3 Relationship between number of large-scale landslides and distance from Yingxiu-Beichuan fault: (a) percentage of large-scale landslides to distance from Yingxiu-Beichuan fault and (b) accumulative percentage of large-scale landslides to distance from Yingxiu-Beichuan fault.

ranks the first which occupied 52.9% of the total surface area of large landslides. It is Area C which contains the landslides with the largest average surface area (617,227 m²) of all five areas. The two largest landslides induced by the Wenchuan Earthquake, the Daguangbao Landslide and the Wenjiagou Landslide are both located in Area C.

Previous research has shown that the fault zone in Yingxiu (Area A) and Beichuan (Area D) suffered the maximum fault displacement during the Wenchuan Earthquake (Xu et al. 2009; Li et al 2009). Field investigations have shown that the ground surface of Qingchuan (Section E in Figure 2) suffered little or no displacement (Xu et al. 2008). The vertical and horizontal surface displacements along the Yingxiu-Beichuan fault are plotted in Figure 4. This figure shows that the concentration areas of large-scale landslides rarely match with

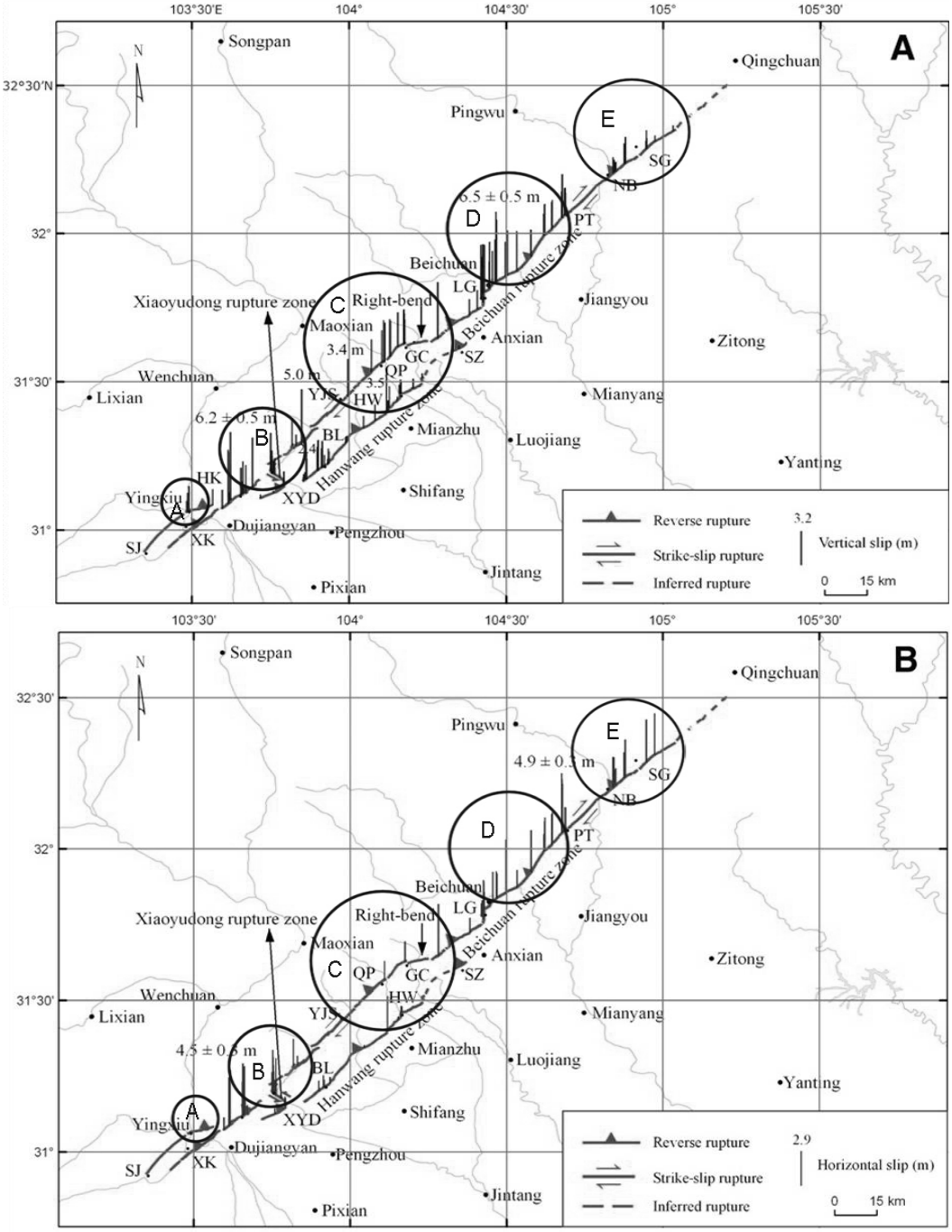

Figure 4 Seismic fault of the Wenchuan Earthquake and its displacement (Xu el al. 2008): (a) relatively vertical displacement of seismic fault; and (b) Horizontal displacement of seismic fault.

zones of maximum magnitude of surface displacements. However, the areas of concentration of large-scale landslides show a good coincidence with the junctions or intersections as well as turning points and ends of the fault segments. Huang and Li (2009) argued that the junctions or intersections and the turning portions were the locally locked segments of the seismic fault, which releases relatively large amounts of energy when they were broken and dislocated by the overall displacement of the fault during the earthquake, working as a secondary "hypocenters". As a consequence, more large-scale landslides occurred near these secondary hypocenters. This phenomenon was clearly exhibited in area C from Qingping to Gaochuan (Figure 2 & Figure 5). Due to the locally staggered arrangement of fault segments the strike-slip movement would have caused high compressive stress at both ends of the staggering section before the earthquake happened (regions of stress concentration in Figure 6). During the earthquake, much energy would be released from these zones leading into the initiation of the two largest landslides in the earthquake affected region (Huang & Li 2009). As shown in Figure 6, the largest landslide, Daguangbao landslide, occurred at one end of the branch of Yingxiu-Beichuan fault while the Wenjiagou landslide (the second largest) is located at the other end of the same fault.

As shown in Table 2, most large-scale landslides in the Wenchuan Earthquake-affected zone were close to the surface rupture zone. Their distances to the seismic fault outcrop were only several hundred meters. For instance, the Donghekou, Woqian, Niumiangou, and Chenjiabaershan landslides were located 300, 200, 300 and 0 m, respectively, away from the seismic fault. However, the largest one, Daguangbao landslide, and the second largest one Wenjiagou landslide were 4800 m and 3900m away from the seismic fault. The same locked segment effect may be the reason for the occurrence of these two landslides despite their relatively long distance from the seismic fault.

As shown in Figure 2, a great number of large-scale landslides developed in Area E where the fault displacements at the surface rupture were not as large as others. The possible explanation may be that the fault zone along the Longmen Mountain Range is developed in several parallel branches in Area E, most of which have undergone only a limited amount of displacement during the Wenchuan Earthquake. This has been concluded

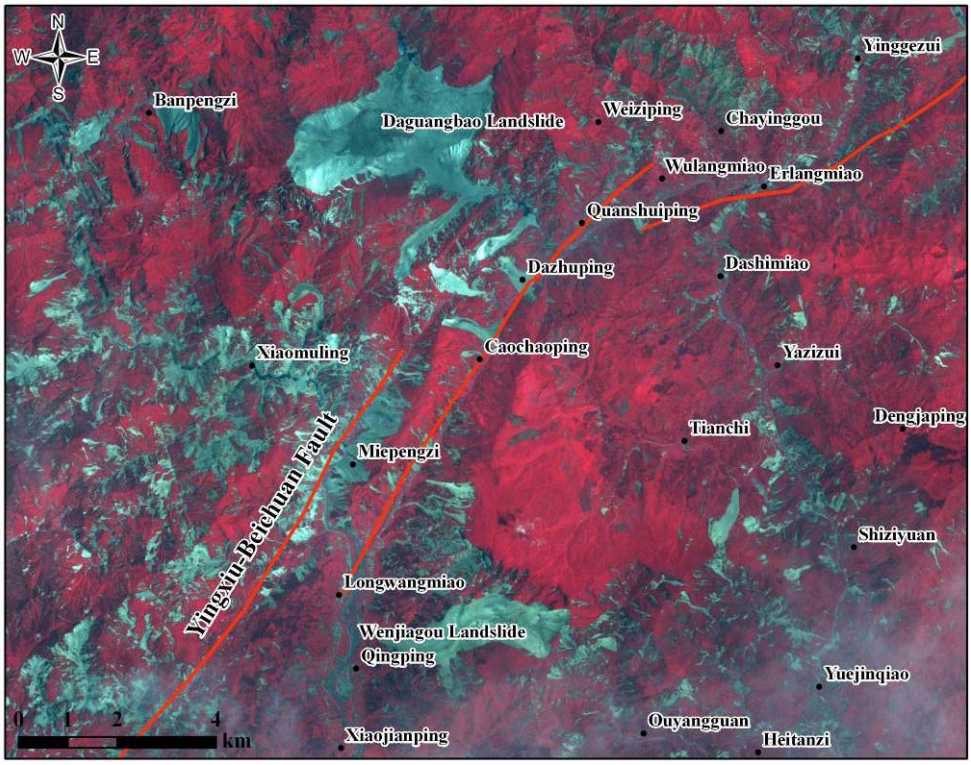

Figure 5 Obvious local dislocation of the fault in Area C

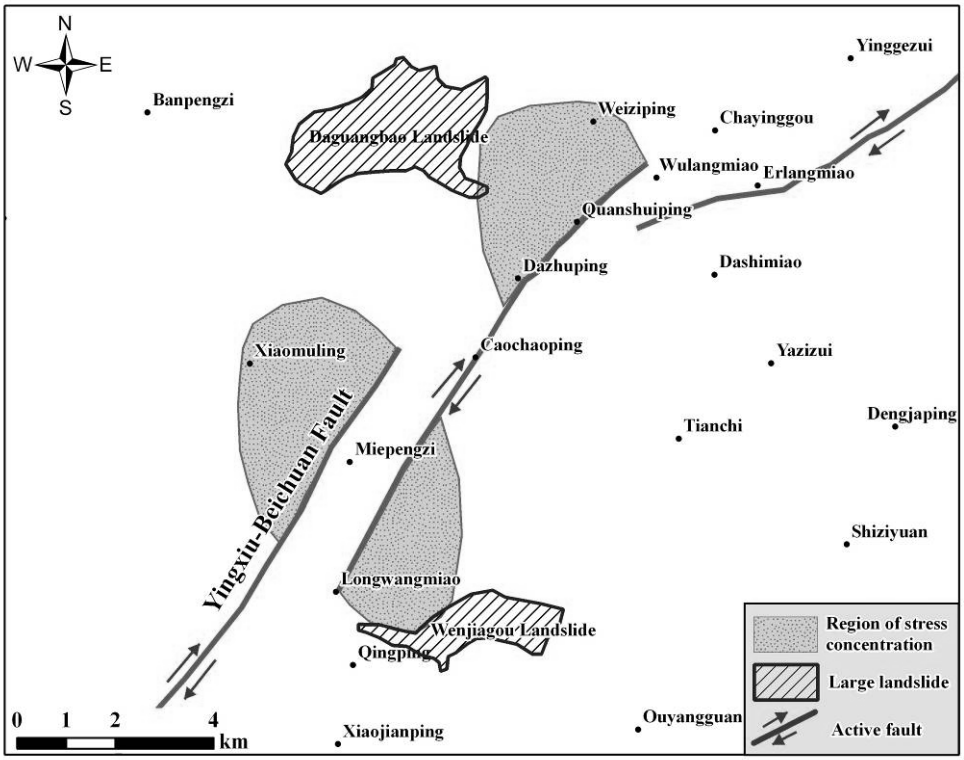

Figure 6 Local stress concentration induced by dislocation of faults in Area C

by the detailed post earthquake field geological survey of the surface ruptures (Li et al. 2009). Remote sensing interpretation and field mapping showed that the distribution of landslides in Area E and the location of branch faults have an obvious correlation (Figure 7).

2.3 Hanging wall effect

Figure 2 and Table 2 show that 80 large-scale landslides out of 112 (71%) were located at the hanging wall side of the seismic fault. Furthermore those large-scale landslides appearing at the footwall side of Yingxiu - Beichuan fault actually were located at the hanging wall side of the Jiangyou-Guanxian fault. In Area E, as mentioned before, a number of branch ruptures were developed. Figure 7, shows that some large-scale landslides were located in the footwall of Jiujiaya-Xiaojingba fault, but they were also on the hanging wall of Beichuan-Chaba fault. Therefore, a vast majority of large-scale landslides was located in the hanging wall of a seismic fault. This is described as the "hanging wall effect."

2.4 Direction effect

The spatial distribution and the sliding direction of landslides show a strong correlation with the geomorphology and the slope structure (Huang & Li 2009). In addition, previous research also indicated that the earthquake dynamics, to

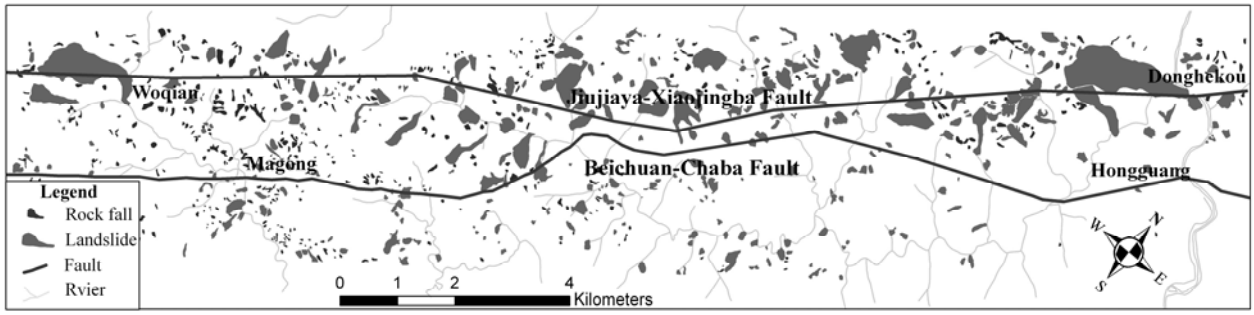

Figure 7 Landslides distribution and fault branches in Area E

some extent, affected the spatial distribution and the sliding direction of earthquake-induced landslides in two ways: back slope effect and partial dislocation of fault segments.

2.4.1 Back slope effect

Based on the landslides induced by the Taiwan Chi-Chi earthquake (MW7.6, 1999) and the Pakistani Kashmir earthquake (MW7.6, 2005), David (2008) argued that the distribution of landslides induced by earthquakes follows the rules of the "hanging wall effect" and the "direction effect". David (2008) indicated that for valleys perpendicular to the seismic fault zone, the slopes facing the seismic source were less susceptible to landslides than the slopes whose dip direction is the same as the travel direction of earthquake waves (Figure8).

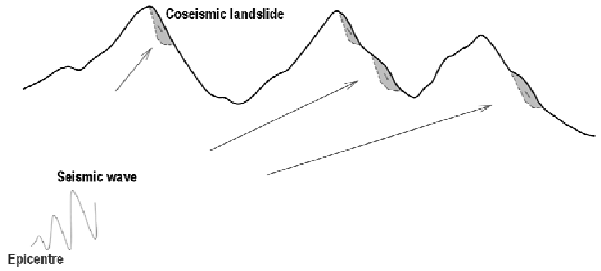

Figure 8 Landslide easily induced at the rear of slope relative to seismic spreading

Tang (2008) suggested that the "back slope effect" might relate to a spalling phenomenon, which is caused by a tension wave generated when a compression wave hits a free surface. The stress wave theory explains that the incident and the reflected wave would be superimposed when an incident wave reaches a boundary. If the stress wave traveling in a solid strikes a free boundary at a normal angle, this will lead to a totally reflected wave at the free boundary. The acceleration and displacement caused by the reflected wave is identical in form to the incident wave and is of the same sign. Superposition of both waves leads to the doubling of the outward acceleration and displacement at the free boundary. So when an earthquake compressive wave hits the free ground surface, it will be reflected as a tensile wave, capable of breaking the rockmass by tension if the tensile stress generated by the reflected wave exceeds the tensile strength of the rocks. When the reflected wave generates a tensile stress more than twice the tensile fracture strength of the rock, several parallel layers of rock may be broken and multiple spalling can occur (Tang 2008).

Near Hongbai Town (to the northwest of Yingxiu Town, the epicenter of Wenchuan Earthquake) there were five northwest striking valleys, perpendicular to the strike of the earthquake seismic fault in the Longmen Mountain Range (Figure 2). The travel direction of the

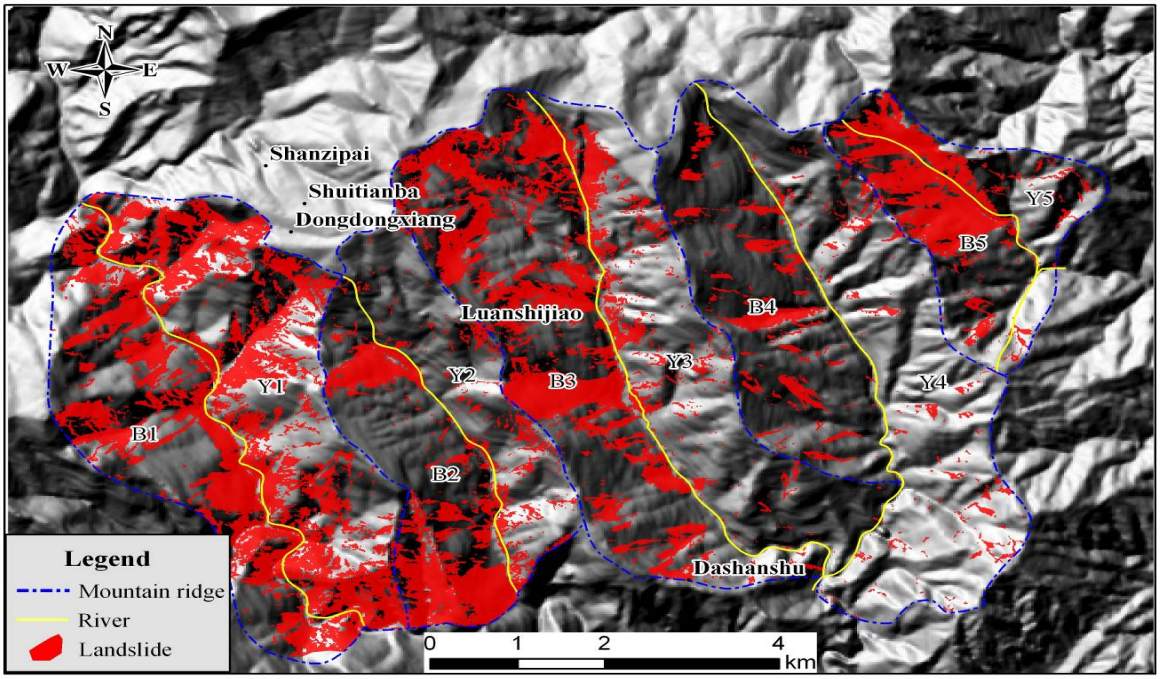

Figure 9 Image interpretation of landslides distribution

seismic wave was perpendicular to the strike direction of these valleys during the earthquake. Two types of slopes were presented along the valleys: back slopes ("B" in Figure 9) and face slopes ("Y"). The back slopes dipped in the same direction as the seismic wave travels while the face slopes dipped towards the source of the seismic wave. The total surface area of each back and face slope and of each landslide was determined from remote sensing imagery and is shown in Table 5. The surface density is defined as the ratio of the landslide covered area to the total area of each slope.

Table 5 and Figure 10 show that the average area density for the back slopes (34.7%) is more than double the area density for face slope (16.9%). These observations are in good agreement with the conclusions from Sato (2009) after studying the Taiwan Chi-Chi earthquake and the Pakistan Kashmir earthquake. The back slope effect is also visible in Yinxing-Futangba section of the Min River (Figure 11) where the landslide density of the right bank of Minjiang River was much higher than that of the left bank. The trend of this section of the river is in almost NS direction, and it is located in the north of the epicenter of the Wenchuan Earthquake zone. Therefore, in the process of seismic wave propagation, right bank slope turned into back slope, while left bank slope turned into face slope.

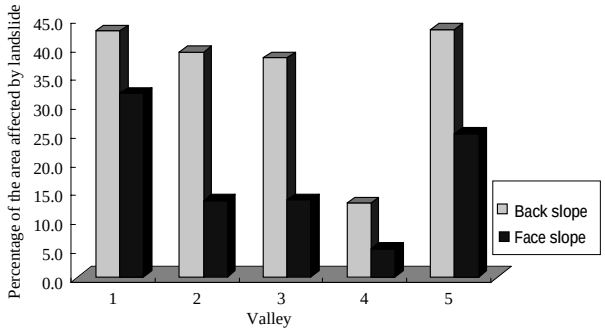

Figure 10 Comparison of area density of landslides on valley slopes

2.4.2 Partial dislocation of fault segments

The southwestern section of the Yingxiu - Beichuan seismic fault predominantly underwent thrusting motion while the northeastern section mainly underwent strike-slip movement (Li et al. 2009). As shown in Figures 2 and 9, landslides usually followed the direction of the valley slope. However, in exceptional cases and especially large-scale landslides, landslide slipped in the direction of seismic wave propagation in the region of Hongshihe River in Qingchuan County (Figure 7). In total, 36 large-scale landslides were located in this area. The number of landslides and their corresponding range of sliding directions are listed in Table 6. A rose diagram was plotted in Figure 12 to show the tendency of sliding directions. There are three predominant groups of sliding directions in this area, Northwest (315°), Southeast (150°) and Northeast (65°). The strike direction of the main valley (Hongshhe River) is parallel with the seismic fault, in NE direction, leading the landsliding directions towards NW and SE at both sides of the valley. The third predominant sliding direction (60°-80°) (Figure 11) is basically the same as the fault strike direction. It should be noted that there are some valley branches perpendicular to the seismic fault, favoring the development of landslides sliding in NE or SW

Figure 11 Wester dipping landslides possess higher density than east dipping landslides in Yinxing-Futangba section of Minjiang River

Table 5 Area of landslides on face slopes and back slopes

Back slope				Face slope			
Zone No.	Landslide area	Total slope area	Surface density	Zone No.	Landslide area	Total slope area	Surface density
B_1	3315679	7750274	42.8	Y_1	2894821	9059926	32.0
B_2	2024665	5168369	39.2	Y_2	600817	4504656	13.3
B_3	4177057	10963506	38.1	Y_3	1036383	7713195	13.4
B_4	887539	6908388	12.8	Y_4	469412	9619007	4.9
B_5	1382774	3205396	43.1	Y_5	690400	2775181	24.9
Total	11787715	33995933	34.7	Total	5691833	33671966	16.9

Table 6 Number of landslides sliding in different directions

Sliding Direction (°)	0~20	20~40	40~60	60~80	80~100	100~120
Number of landslides	2	1	3	5	2	1
Sliding Direction (°)	120~140	140~160	140~180	180~200	200~220	220~240
Number of landslides	0	5	2	1	1	1
Sliding Direction (°)	240~260	260~280	280~300	300~320	320~340	340~360
Number of landslides	1	0	0	4	2	5
Note: 0° denotes the north direction and increases clockwise.						

direction. However, compared with the 10 landslides sliding NE, only 3 landslides slipped SW. This may be due to the horizontal twisting and staggering motion of the seismic fault in this area.

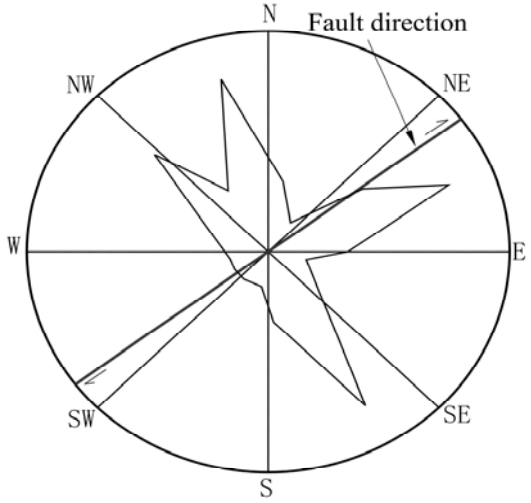

Figure 12 Rose diagram showing the motion direction of large-scale landslides along Hongshi River

4 Conclusions

Based on the analysis of the spatial distribution of the large-scale landslides (surface area > 50,000 m^2) induced by the Wenchuan Eearthquake from remote sensing interpretation and field investigation, the following conclusions were drawn:

(1) Distance effect. Large-scale landslides were concentrated within a certain limited distance at both sides of the surface outcrop of the seismic fault. About 40% of the large-scale landslides were located within 1 km; 70% landslides within 3 km; and more than 80% within 5 km from the fault outcrop. Beyond a distance of 13 km, no large-scale landslide occurred.

(2) Locked segment effect. Large-scale landslides triggered by the Wenchuan Earthquake were found to be concentrated in the Areas A, B, C, D, and E (see Figure 2). The zone with the highest concentration was Area C, where the two largest landslides were located. These concentration zones coincided with the locked segments of the Yingxiu-Beichuan fault, with staggering, dislocation and rupture phenomena. Large amount of energy was released in these areas due to the rupture and displacement of the seismic fault.

(3) Hanging wall effect. More than 70% of the large-scale landslides were identified on the hanging wall of the seismic fault. This may be related to the higher peak acceleration in the hanging wall.

(4) Direction effect. The slopes dipping towards the source of earthquake wave were found to be less susceptible to large-scale landslides than the slopes whose dip direction was the same as the travel direction of the seismic wave. The sliding

directions of the large-scale landslides were found to coincide with the staggering direction of the seismic fault in each section.

Acknowledgements

This study was sponsored by the project of the Chinese National Key Basic Research Program on "The failure mechanism and distribution rule of slopes under strong earthquakes" (Grant No. 2008CB425801), the Education Department Innovation Research Team Program (Grant No. IRT0812) and standed as an independent research topic of Geo-hazard Prevention and Geoenvironment Protection on "The research on large-scale landslides induced by the Wenchuan Earthquake". Many thanks are owed to the PhD students involved in this study for their data collection and field investigation. The authors also give great thanks to Dr. Niek Rengers and Dr. Yan R. Li for their kindly checking and polishing the language, which greatly improved the quality of the manuscript.

References

Champati RPK, Parvaiz I (2009) Analysis of seismicity-induced landslides due to the 8 October 2005 earthquake in Kashmir Himalaya. Current science 97 (12): 1742-1751

Cole WF, Marcum DR,Shires PO (1998) Analysis of earthquake-reactivated landslides in the epicenter region, central santa crumountains, California. In: Keefer DV (eds.), The Loma Prieta,California,Earthquake of October 17,1989-Landslides:U.S. Geological Survey Professional paper1551-C. pp C165-C185

David P (2008) Earthquake induced landslides lessons from Taiwan and Pakistan. In: Multi-media academic report in Chengdu University of Technology.

Garcia-Rodriguez MJ, Malpica JA, Benito B (2008) Susceptibility assessment of earthquake-triggered landslides in El Salvador using logistic regression. [Retrieved on November 6, 2010 from http://oa.upm.es/2325/1/INVE_MEM_2008_54925.pdf]

Hasi B, Ishii Y, Maruyama K, et al. (2010) Controls on distribution and scale of earthquake-induced landslides caused by the Iwate-Miyagi Inland earthquake in 2008, Japan. European Geosciences Union (EGU) General Assembly 2010, held 2-7 May, 2010 in Vienna, Austria. p 3827

Hasi B, Ishii Y, Suzuki S et al. (2009) Landslides distribution nearby earthquake seismic fault of the Chuetsu-offshore earthquake, Niigata Prefecture in 2007. [Retrieved on November 6, 2010 from http://wwwsoc.nii.ac.jp/jepsjmo/cd-rom/2009cd-rom/program/session/pdf/Y167/Y167-P003_e.pdf]

Huang RQ et al. (2009) Geohazard Assessment of the Wenchuan earthquake. Beijing: Science Press. (In Chinese)

Huang RQ, Pei XJ, Li TB (2008a) Basic characteristics and formation mechanism of the largest-scale landslide at Daguangbao occurred during the Wenchuan Earthquake. Journal of Engineering Geology 16(6): 730-741.(In Chinese)

Huang RQ, XU Q et al. (2008b) Catastrophic landslides in China. Beijing: Science Press. (In Chinese)

Huang RQ, Li WL (2008) Research on development and distribution rules of geohazards induced by Wenchuan earthquake on 12th May,2008. Chinese Journal of Rock Mechanics and Engineering 27(12): 2585-2592. (In Chinese)

Huang RQ, Li WL (2009) Fault effect analysis of geo-hazard triggered by Wenchuan earthquake. Journal of Engineering Geology 17 (1): 19-28.(In Chinese)

Jibson RW, Harp EL, Michael JA (1998) A method for producing digital probabilistic seismic landslide hazard maps: an example from the Los Angeles, California, area. U.S. Geological Survey Open-file Report: 98-113

Keefer DK (1984) Landslides caused by earthquakes. Geological Society of America Bulletin, 95: 406-421

Li CY, Wei ZY (2009) Deformation styles of the northernmost surface rupture zone of the MS 8.0 Wenchuan earthquake. Seismology and Geology 31(1): 1-8.(In Chinese)

Li Y，Huang RQ et al. (2009) Basic features and research progresses of Wenchuan Ms 8.0 earthquake. Journal of Sichuan University (Engineering Science edition) 41(3): 7-25. (In Chinese)

Marui H Landslide Disaster Caused by Inland Earthquake. [Retrieved on November 6, 2010 from http:/ /www.sabo-int.org/case/2007pakistan.pdf]

McCrink TP and Real CR (1996) Evaluation of the Newmark method for mapping earthquake-induced landslide hazards in the Laurel 7.5' quadrangle, Santa Cruz County, California.California Division of Mines and Geology Final Technical Report for U.S. Geological Survey Contract 143-93-G-2334, U.S. Geological Survey, Reston Virginia, p31

Ramos-C, AM,Rodriguez-P, C. E (2009) Ground strong motion and landslides relationships: the lamaprieta earthquake analysis. [Retrieved on November 6, 2010 from http://fing.javeriana.edu.co/ geofisico/ ARCHIVOS/ 8NCEE-0251.pdf]

Sato HP, Harp EL (2009) Interpretation of earthquake-induced landslides triggered by the 12 May 2008, M7.9 Wenchuan earthquake in the Beichuan area, Sichuan Province, China using satellite imagery and Google Earth. Landslides 6:153-159

Tang CA, Zuo YJ, Qin SF et al. (2008) Landslide shallow layer spalling cast modes and its kinetics explanation in Wenchuan earthquake. In: Song SW (eds.), The proceedings of the tenth national rock mechanics and engineering science conference, Chengdu, China. pp 258-262. (In Chinese)

Westen CV, Gorum T, Fan XM et al. (2010) Distribution pattern of earthquake-induced landslides triggered by the 12 May 2008 Wenchuan Earthquake. Geophysical Research Abstracts 12.(EGU2010-4437)

Wang J, Yao LK, Arshad H (2010) Analysis of earthquake-triggered failure mechanisms of slopes and sliding surfaces. Journal of Mountain Science 7:282-290

Xu C, Dai FC, Yao X (2009) Incidence number and affected area of Wenchuan Earthquake-induced landslides. Review of Science and Technology 27(11): 79-81 (In Chinese)

Xu Q, Huang RQ (2008) Kinetics characteristics of large landslides triggered by May 12th Wenchuan earthquake. Journal of Engineering Geology 16(6): 721-729. (In Chinese)

Xu Q, Pei XJ, Huang RQ et al. (2009) Large-scale landslides induced by the Wenchuan earthquake. Science Press. (In Chinese)

Xu XW, Wen XZ, Ye JQ et al. (2008) The MS 8.0 Wenchuan earthquake surface ruptures and it's seismogenic structure. Seismology and geology 30(3): 597-628. (In Chinese)